Locally triggered seismicity in the central Swiss Alps following the large rainfall event of August 2005

S. Husen, C. Bachmann and D. Giardini

Swiss Seismological Service, Schafmattstrasse 30, *ETH Zurich,* CH8093 *Zurich, Switzerland. E-mail: shusen@sed.ethz.ch*

SUMMARY

In 2005 August, an unusual series of 47 earthquakes occurred over a 12-hr period in central Switzerland. The earthquakes occurred at the end of 3-d period of intensive rainfall, with over 300 mm of precipitation. The highest seismicity occurred as two distinct clusters in the region of Muotatal and Riemenstalden, Switzerland, a well-known Karst area that received a particularly large amount of rainfall. The large increase in seismicity, compared to the background, and the short time delay between the onset of the intense rainfall and the seismicity strongly suggest that earthquakes were triggered by rainfall. In our preferred model, an increase in fluid pressure at the surface due to a large amount of rain leads to a local increase in pore fluid pressure at depth. The increase in pore fluid pressure will reduce the shear strength of a porous medium by counteracting normal stress and, at the end, provoke failure. The series of triggered earthquakes in central Switzerland occurred in regions that have been seismically active in the past, showing similar hypocentre locations and magnitudes. This suggests that these earthquakes occurred on existing faults that were critically stressed. We modelled the intense rainfall as a step increase in fluid pressure at the surface that migrates to greater depths following the solution of the one-dimensional diffusion equation in a homogeneous half space. This allowed us to estimate the hydraulic diffusivity by plotting triggered seismicity in a time–depth plot. We found values of hydraulic diffusivity in the range from 0.01 to 0.5 m^2 s^{-1} for our study area. These values are in good agreement with previous studies on earthquakes that were triggered by fluids, supporting the idea that the observed earthquake series was triggered by the large amount of rainfall.

Keywords: Alps, induced seismicity, rainfall, Switzerland.

GJI Seismology

INTRODUCTION

Fluids play an important role in triggering local earthquakes. There are a number of examples, where changes in pore fluid pressure, either natural or man-made, triggered earthquakes. This process is also known as hydroseismicity. Well-known examples of hydroseismicity include seismicity induced by reservoir filling (Talwani & Acree 1984; Gupta 2002), or by forced fluid injection at depth (Aki *et al.* 1982; Zoback & Harjes 1997; Phillips 2000). Examples of naturally induced changes in pore pressure that lead to earthquake triggering are rare and subtle. Periods of elevated seismicity induced by seasonal groundwater recharge (Roth *et al.* 1992; Saar & Manga 2003) or following intense rainfall are good examples of the latter (Jimenez & Garcia-Fernandez 2000; Hainzl *et al.* 2006; Kraft *et al.* 2006). It has been also suggested that aftershocks are driven fluid flow (Nur & Booker 1972; Miller *et al.* 2004). Hydroseismicity may also be caused by the passage of low-frequency, large-amplitude surface waves of distant earthquakes, a phenomena called dynamic earthquake triggering (Husen *et al.* 2004; Prejean *et al.* 2004). Despite the, usually, small magnitudes of triggered earthquakes, their study

can provide insights into the state of stress and into the hydraulic properties of the uppermost crust.

In this study, we present observations on a series of local earthquakes in the central Alps, Switzerland that followed a period of intense rainfall. During the time period August 19–August 23, 2005, some of the largest rainfall ever recorded occurred in central Switzerland. Within 4 d, over 300 mm of rain felt over a wide region in central Switzerland (Fig. 1). An unusual series of 47 earthquakes occurred over a 12-hr period at the end of the rainfall event. Most of the earthquakes clustered in a region around Lake Lucerne (Fig. 1), which is a well-known Karst area in the central Alps of Switzerland. We model the intense rainfall as a step increase in fluid pressure at the surface that migrates to greater depths following the solution of the 1-D diffusion equation in a homogeneous half space. This allows us to estimate the hydraulic diffusivity by plotting triggered seismicity in a time–depth plot. We find values of hydraulic diffusivity in the range from 0.01 to 0.5 m^2 s^{-1} for our study area. These values are in good agreement with previous studies on hydroseismicity, supporting the idea that the observed earthquake series was triggered by the large amount of rainfall.
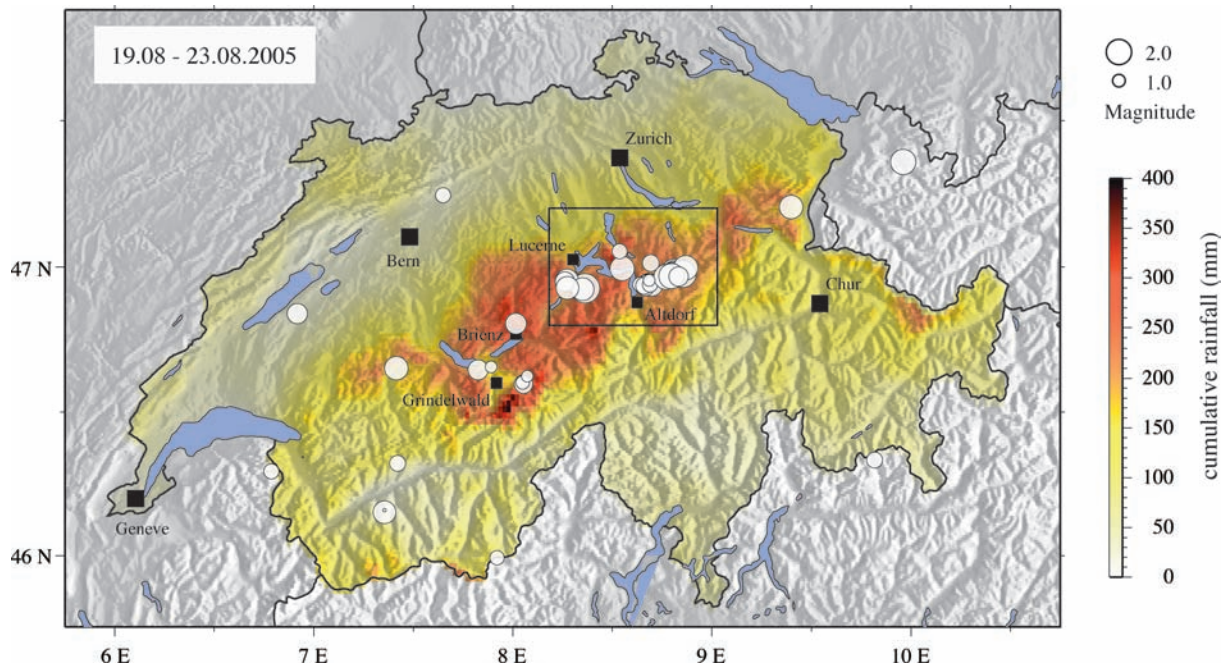
Figure 1. Cumulative rainfall (colour coded in online version) and observed seismicity (white circles) in Switzerland for the time period 08/19/2005–08/23/2005. Size of circles is scaled by magnitude as indicated. Black rectangle outlines area shown in Fig. 2.

OBSERVATIONS

Rainfall

Between August 19 and 23, 2005, a low-pressure system moved northwards from the Gulf of Genoa, northern Italy, towards the eastern Alps, Austria. With the low-pressure system warm and moisture air from the Mediterranean was moved across the Alps and back to the Alps, where it was pushed against the northern Alps. This lead to intense rainfall across central Switzerland, which set new records at many sites of the Meteoswiss network, the Swiss Weather Service, monitoring precipitation in this area. Within 48 hr over 150 mm of rain was recorded. The statistical recurrence rate for such high rainfall is more than 300 yr (Meteoswiss 2005, personal communication), which clearly emphasize the exceptionality of the amount of rain recorded. On top of the large rainfall, soil in central Switzerland was already saturated before the onset of the rain-event, due to an unusual wet August. This lead to an immediate increase in discharge rates of streams and rivers, which caused substantial flooding and landslides in central Switzerland.

Meteoswiss operates three stations for continuous monitoring of precipitation in the region around Lake Lucerne, central Switzerland. At all stations, data was taken automatically every hour. In this study, we will show data of the station Altdorf, which is closest to the observed clusters of earthquakes (Fig. 1). In addition to data from the Meteoswiss, data are also available from two stations, Schlichenden Brünnen and Twäreren, operated by the Hoelloch Cave Research Association (Fig. 2). These stations monitor precipitation and discharge (only Schlichenden Brünnen) at the Hoelloch cave, with its estimated length of 190 km one of the largest caves in Karst terrain in Europe (Boegli 1970). Both stations are close to the village Muotathal, where we observe the most intense seismicity following the rainfall. Fig. 3 compares precipitation for stations Twären, Schlichenden Brünnen and Altdorf in the time period 08/19/2005 to 08/24/2005. All three stations show the same rainfall pattern with a first, small, maximum in precipitation between 08/19/2005 and
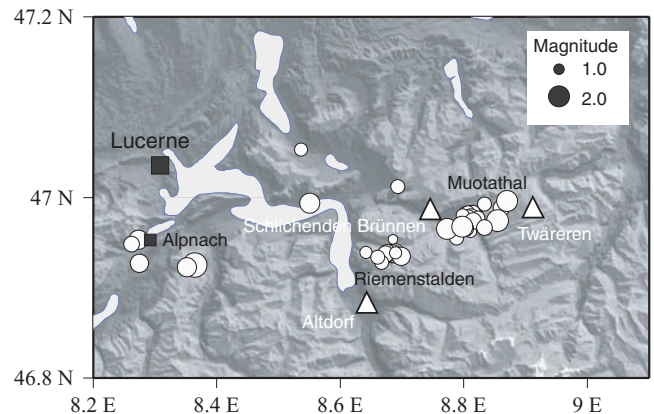

Figure 2. Observed seismicity (white circles) in the region of Lake Lucerne. See Fig. 1 for location of area. Locations of meteorological stations, for which data (rainfall and discharge) was available, are marked by white triangles. Regions with highest seismicity (Riemenstalden and Muotathal) are labelled.

08/20/2005. The second phase started on 08/21/2005, which lasted until 08/23/2005 with a small break in precipitation at the end of day 08/21/2005. The maximum in precipitation is reached between 08/22/2005 and 08/23/2005 for stations Twäreren and Schlichenden Brünnen; in Altdorf the peak in precipitation is reached at the end of day 08/21/2005. The largest amount of precipitation was recorded at station Twäreren, with more than 250 mm rain between 08/19/2005 and 08/24/2005 (Fig. 3); at stations Schlichenden Brünnen and Aldorf a total of nearly 200 mm rain and 150 mm rain were recorded, respectively. Since all three stations show the same characteristics in precipitation, we decided to use data from Schlichenden Brünnen to estimate the time lag between the onset of precipitation and seismicity. Station Schlichenden Brünnen is located close to the main cluster of seismicity following the rainfall. In addition, discharge data is also available for the same station.
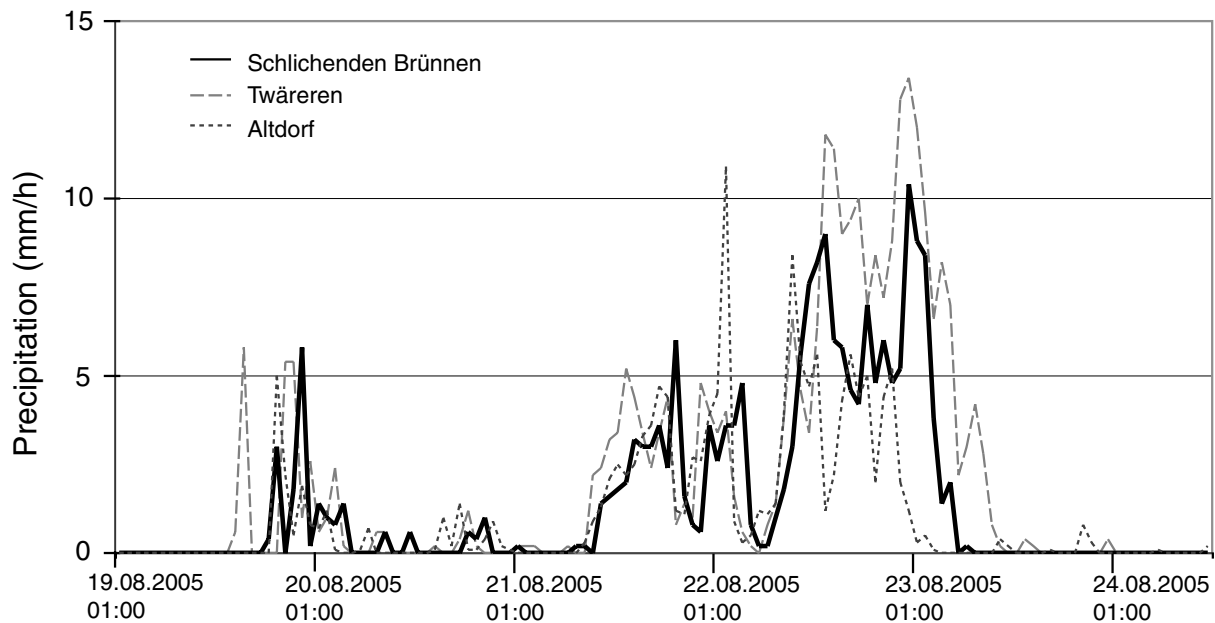
Figure 3. Precipitation (rainfall) at stations Schlichenden Brünnen (solid line), Twäreren (dashed line) and Altdorf (heavy dashed line) for time period 08/19/2005–08/25/2005. Data for Schlichenden Brünnen and Twäreren were taken at 30 min intervals; data for Altdorf were taken at hourly intervals. Stations Schlichenden Brünnen and Twäreren are operated by the Hölloch Cave Research Association (Swiss Hydrological Survey 2007); station Altdorf is operated by MeteoSwiss.
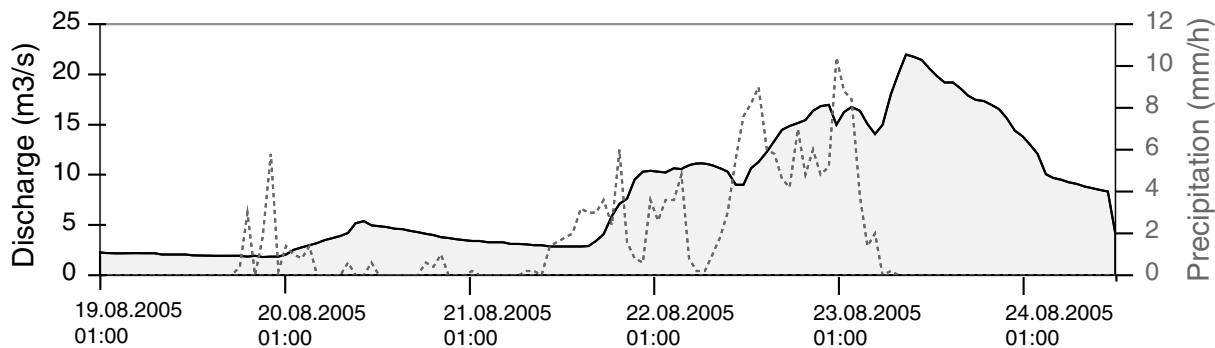
Figure 4. Precipitation (dashed line) and discharge at station Schlichenden Brünnen operated by the Hölloch Cave Research Association (Swiss Hydrological Survey 2007). Data was taken at 30 min intervals for the time period 08/19/2005–08/25/2005. Discharge data after 08/24/2005 is unreliable due to damage at the station.

Among precipitation, the station Schlichenden Brunnen also recorded discharge of the river Schlichenden Brunnen, which is the main outflow of the Hoelloch cave (Fig. 4). Unfortunately, the station was heavily damaged by the large amount of water, so that discharge data is only reliable until 08/24/2005. The peak in discharge occurred at the middle of day 08/23/2005, clearly delayed by a few hours compared to the maximum in precipitation (Fig. 4). Using a total of 200 mm precipitation between 08/19/2005 and 08/23/2005 measured at station Schlichenden Brunnen and a catchment area of 30 km^2 for the Karst area that drains through the Hoelloch cave (Wildberger and Baettig, in press) we estimate a total volume of 6 Mio m^3 of water that entered the Hoelloch cave. Between 08/22/2005 and 08/23/2005, at the peak discharge, about 2.5 Mio m^3 of water were drained through Schlichenden Brunnen. An additional 0.5–0.7 Mio m^3 were likely drained through secondary drainages that are not monitored (Wildberger and Baettig, in press). Although our estimates are a rather crude approximation, the discrepancy between precipitation and drainage

suggests that a substantial part of the water infiltrated the uppermost crust.

Seismicity

The Swiss Seismological Service operates a seismic network to monitor ongoing seismicity in Switzerland. In 2005, the network consisted of 36 digital stations, most of them equipped with broadband STS2 sensors. Data is recorded continuously and streamed in real-time to the data centre of the Swiss Seismological Service in Zurich, where it is routinely processed. For earthquake location, a 3-D *P*-wave velocity model is used, which is based on available controlled-source seismological data and local earthquake data (Husen *et al.* 2003). For *S*-wave arrivals a constant *P*- to *S*-wave ratio of 1.71 is used. Hypocentre locations are determined using the software package NonLinLoc (Lomax *et al.* 2000). NonLinLoc computes the posteriori probability density function (PDF) using either a systematic grid-search on nested grids or a global

importance sampling algorithm, called Oct-Tree. In this study, we use the Oct-Tree importance sampling algorithm, which provides accurate and efficient mapping of the PDF (Husen *et al.* 2003). The PDF represents a complete, probabilistic solution to the earthquake location problem, including complete information on location uncertainties and resolution (Lomax *et al.* 2000). Location uncertainties can be either shown using density scatter clouds or by the 68 per cent confidence ellipsoid (Husen *et al.* 2003). For well-posed location problems, i.e. at least six observing stations and an azimuthal gap <180°, the 68 per cent confidence ellipsoid is a good approximation to the true location uncertainties, which can be highly irregular. In this study we will show the 68 per cent confidence ellipsoid since all our hypocentre locations are relatively well constrained.

Between 08/19/2005 and 08/23/2005 the Swiss Seismological Service located 53 earthquakes in Switzerland and surrounding regions (Fig. 1). Most of the earthquakes occurred in the region around Lake Lucerne, which also received some of the highest rainfall. A few earthquakes occurred in the region around Grindelwald, BE, which also received a high amount of rainfall. Although rainfall was as high, the region between Lake Lucerne and Grindelwald was seismically quiet, except one earthquake that occurred close to Brienz (Fig. 1). Local magnitudes of the earthquakes ranged from 1.0 to 2.4 (Figs 1 and 2); some of them were felt locally, indicating very shallow focal depths. A few earthquakes occurred in regions with low rainfall, which likely represent normal background seismicity (Fig. 1). In contrast, the Swiss Seismological Service located five earthquakes between 08/14/2005 and 08/18/2005; none of them occurred in central Switzerland.

Earthquakes in central Switzerland between 08/19/2005 and 08/23/2005 occurred preferentially within the Helvetic nappes (Fig. 5). The Helvetic nappes originated from the margin of the Eurasian continent, and have been folded extensively during crustal shortening, that concentrated mainly along the Penninic frontal thrust in the early Miocene (Schmid & Kissling 2000). The geology of the Helvetic nappes is dominated by limestone sediments with distinct signs of Karst formation (Schmid *et al.* 2004). For example, one of the largest limestone caves in Europe, the Hoelloch cave, is located in the region of Muotathal and Riemenstalden (Boegli 1970). In contrast, no earthquakes occurred in the Molasse basin of the Alpine foreland, although the region close to the central Alps received a substantial amount of rainfall (Fig. 1).

The highest seismicity occurred as two distinct clusters in the region of Muotathal and Riemenstalden (Figs 2 and 6). Focal depths of these earthquakes were shallow, between the surface and 5 km depth. Most of the earthquakes, however, have large uncertainties in focal depth due to a low number of observations, a consequence of their small magnitudes. Only a few larger events with ML > 2.0 are fairly well constrained in focal depth (Fig. 6). Both regions, Muotathal and Riemenstalden, have been seismically active in the past. Seismicity following the rainfall occurred close to locations of previous earthquakes (Fig. 6). Because seismicity in the region of Muotathal and Riemenstalden clustered closely in time and space we used waveform cross-correlation to identify clusters of similar waveforms (Rowe *et al.* 2002). For Riemenstalden we found two distinct clusters of similar waveforms that contained 70 per cent of the recorded seismicity; for Muotathal no clear clustering in waveforms was found. The results suggest that in Riemenstalden two main source regions were active, whereas for Muotathal either different source regions were active or a few main source regions produced events with different focal mechanisms. Given the tight clustering in hypocentre locations for events in Muotathal the latter scenario
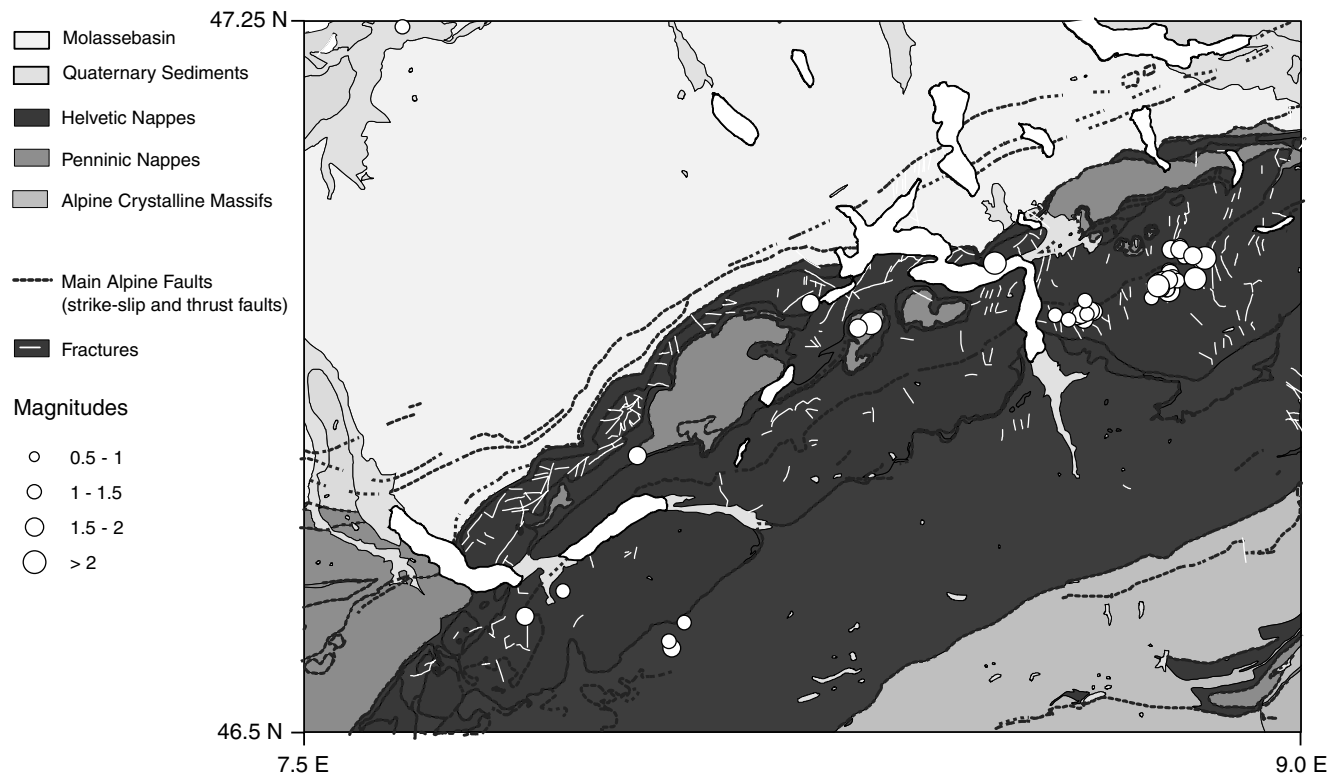
Figure 5. Principal tectonic units of central Switzerland (modified from Schmid *et al.* 2004). White circles denote epicentre locations of earthquakes for the time period 08/19/2005–08/23/2005. Size of circles is scaled by magnitude as indicated.
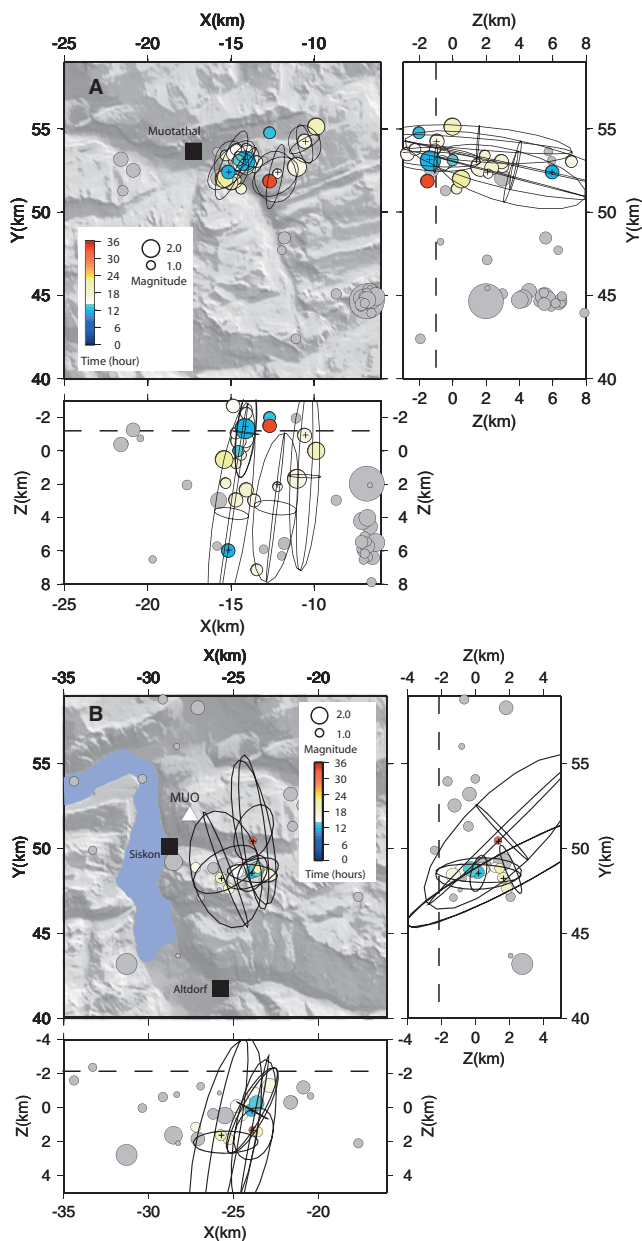
Figure 6. Hypocentre locations (circles) of earthquakes in the time period 08/19/2005–08/25/2005 for regions (a) Muotathal and (b) Riemenstalden. Circles are coded in grey colours (colour in online version) by time (hours since 08/22/2005 12:00). Background seismicity (1999–2004) is shown with open (grey in online version) circles. For a few representative examples uncertainties in hypocentre locations are shown by the 68 per cent confidence ellipsoid. See text for details on how hypocentre locations and confidence ellipsoids were computed. Dashed lines in vertical depth sections mark average elevation of the surface at the epicentre locations. White triangle marks station MUO of the Swiss Digital Seismological Network.

is likely. Unfortunately, the low number of observations does not allow to compute reliable focal mechanisms for these events.

RESULTS

For both regions, Muotathal and Riemenstalden, the observed seismicity following the rainfall was unprecedented. Although both regions are seismically active, the intensity of earthquake activity, i.e.

number of earthquakes per time, following the rainfall was unique since 1999 (Fig. 7). Data before 1999 is difficult to compare with due to a significant network upgrade that started in 1999. As a consequence, sensitivity and hypocentre location accuracy was significantly increased in the study region yielding data sets with different magnitudes of completeness and hypocentral distributions prior and after 1999. Starting 08/22/2005, 37 earthquakes could be located in the Muotathal and Riemenstalden area over a 12-hr period. Given a background rate of two earthquakes per day in all Switzerland, this is equivalent to an increase in seismicity by a factor of roughly 400.

The large increase in seismicity and the short time delay between the onset of the intense rainfall and the seismicity strongly suggest that earthquakes were triggered by rainfall. Rainfall started on 08/19/2005 at 18:00; the first earthquakes occurred in the Muotathal region on 08/22/2005 at 22:00 and on 08/23/2005 at 00:00 in the Riemstaldental region (Fig. 7). This corresponds to a time delay of 76 hr (=3.2 d) and 78 hr (=3.25 d) for the Muotathal region and the Riemenstalden region, respectively. Time lags between the onset of the triggering event and seismicity can range from a few days for rainfall induced earthquakes to a few months for seismicity induced by seasonal groundwater recharge. For example, triggered seismicity following periods of intense rainfall in the Mount Hohenstaufen region, SE Germany, was delayed on average by 10 d (Kraft *et al.* 2006). For the eastern Swiss Alps, an earlier study of the seasonal variation of seismicity found a time lag of about 2 months between the maximum in water flux at the surface and the maximum in earthquake activity per month (Roth *et al.* 1992). Another well documented case of seismicity induced by seasonal groundwater recharge at Mt Hood, Oregon, estimated a time lag of about 151 d (Saar & Manga 2003). The situation at Mount Hohenstaufen shows strong similarities to our observations. In both cases, periods of intense rainfall were followed by increased earthquake activity within a few days. Both regions predominantly consist of limestone and dolomite with distinct signs of Karst formation. And both regions have been seismically active indicating that they are tectonically pre-stressed.

A common concept to explain hydroseismicity is that an increase in pore fluid pressure reduces the shear strength of a porous medium by counteracting normal stress (Saar & Manga 2003; Shapiro *et al.* 2005). In the framework of Coulomb failure, an increase in pore fluid pressure moves the Mohr circle closer to the Mohr–Coulomb failure envelope, while leaving the material's shear strength unchanged. If a porous medium is stressed to near critically values even a small increase in pore pressure can provoke failure (Saar & Manga 2003; Hainzl *et al.* 2006). Changes in pore pressure as a triggering mechanism for earthquakes have been postulated for many studies; for example, aftershock series (Nur & Booker 1972; Miller *et al.* 2004), earthquake swarms (Parotidis *et al.* 2005), reservoir induced and fluid-injection induced earthquakes (Talwani 1997; Zoback & Harjes 1997), microseismicity related to seasonal changes in groundwater flow or stream discharge (Roth *et al.* 1992; Saar & Manga 2003) and earthquakes following periods of intense rainfall (Jimenez & Garcia-Fernandez 2000; Hainzl *et al.* 2006; Kraft *et al.* 2006).

In this study, we also assume that an increase in pore fluid pressure due to the infiltration of large amounts of rain is a viable mechanism to explain the observed increase in seismicity. Pressure diffusion of a large pressure impulse, caused by intense rainfall at the surface, may lead to a local increase in pore fluid pressure at depth. A common characteristic of hydroseismicity is that earthquakes often occur after a certain time lag, that is related to the hydraulic diffusivity (Talwani & Acree 1984). We observed a time delay of 76
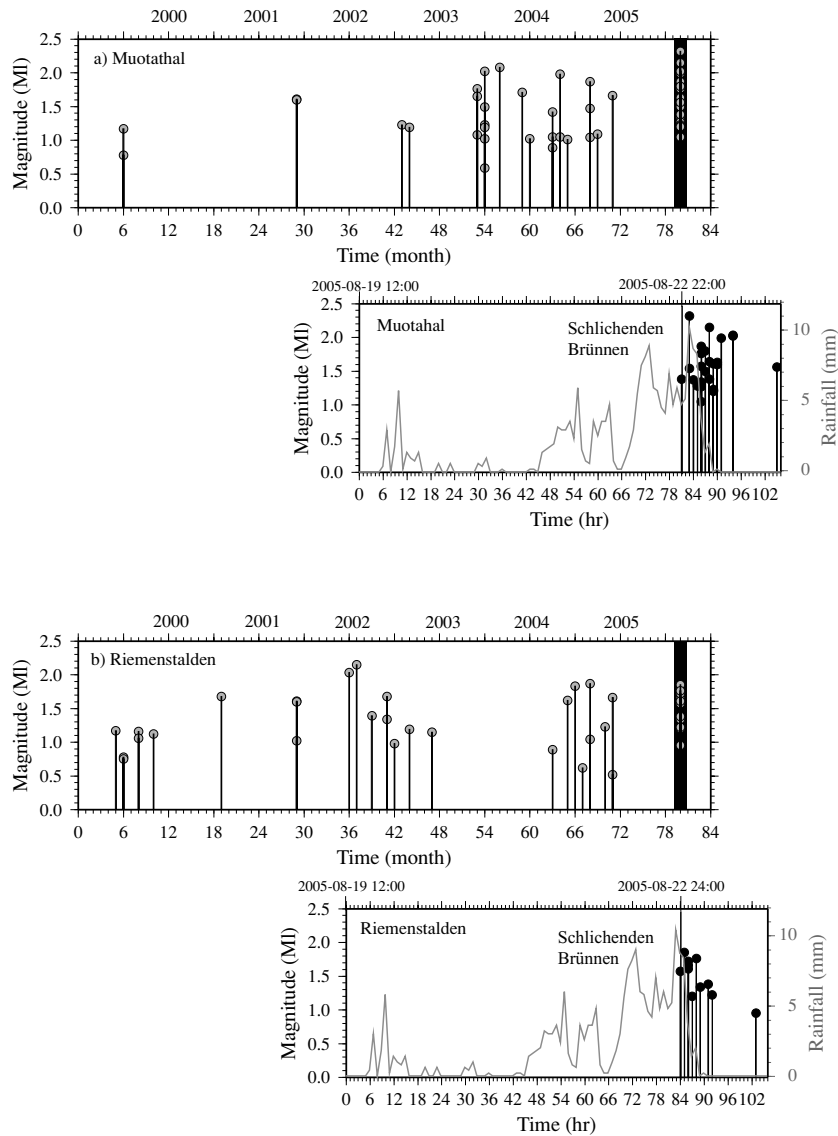
Figure 7. Earthquake magnitude (Ml) versus time for time period 1999–2006 (top) and for time period 08/19/2005–08/24/2005 (bottom) for (a) Muothatal and (b) Riemenstalden region, respectively. Precipitation data at station Schlichenden Brünnen is shown in lower plot.

and 78 hr, for the Muotathal region and the Riemenstalden region, respectively, between the first onset of the rainfall the occurrence of the first earthquakes. If pore pressure diffusion is the dominating process then the observed time lag should correspond to a reasonable estimate of the hydraulic diffusivity. The following rough estimate of the hydraulic diffusivity D is often used to compute D from the distance L of a triggered earthquake to the fluid source and the time lag Δt (Talwani & Acree 1984):

$$D \approx L^2 / \Delta t. \qquad (1)$$

Because eq. (1) often overestimates D we chose a more realistic approach to estimate D, first presented by Shapiro *et al.* (1997). In this approach, pore pressure diffusion is modelled in an infinite homogeneous isotropic poroelastic saturated medium; the initial pore-pressure pertubation (rainfall) is given by a step increase in fluid pressure at the surface of the medium. Since triggered seismicity is clustered in space and time, we use focal depth as distance and consider the initial pore-pressure pertubation as a point source.

In a source free, homogeneous half space, with scalar hydraulic diffusivity D, the low-frequency evolution of pore pressure P due to irrotational flow can be described by the diffusion equation (Shapiro *et al.* 1997; Wang 2000):

$$\frac{\partial P}{\partial t} = D\nabla^2 P. \qquad (2)$$

For a periodic pore-pressure variation $P(0,t) = P_s \exp(i\omega t)$ at the surface of the half space the solution to eq. (1) is given by (Wang 2000; Kraft *et al.* 2006):

$$P(z, t) = P_s \exp\left(-z\sqrt{\frac{\omega}{2D}}\right) \exp\left[i\omega\left(t - \frac{2}{\sqrt{2\omega D}}\right)\right]. \qquad (3)$$

This is a plane wave with attenuation coefficient equal to $\sqrt{2\omega D}$ and with a velocity of $\sqrt{2\omega D}$, where z is depth, t is time, and ω is angular frequency.

To estimate the hydraulic diffusivity D from eq. (3) we follow the logic of Shapiro *et al.* (1997) and Kraft *et al.* (2006): The increase in pore pressure at the surface can be modelled as a rectangular

pressure pulse starting at the same time as the rainfall $t = 0$ and ending at some time $t = t_e$. For an earthquake triggered at time $t = t_0$ the evolution of the pressure pulse for times $t > t_0$ is irrelevant. Consequently, the duration of the pressure pulse can be set to t_0 for this event. The dominant frequencies of the power spectrum of a rectangular pulse with duration t_0 are in the range $0 \leq \omega \leq 2\pi/t_0 = \omega_0$. The propagation velocity of pore-pressure variations is proportional to $\sqrt{\omega}$ (eq. 3). Assuming that even small increases in pore fluid pressure can trigger seismicity, we set $\omega = \omega_0 = 2 - \pi/t_0$ to calculate the velocity of a pressure front behind which seismicity can be triggered. For the time range $t_0 \in [0,t]$ we find the time–depth dependence of the triggering pressure front as (Kraft *et al.* 2006):

$$z = \sqrt{4\pi Dt}. \qquad (4)$$

By plotting focal depth of triggered earthquakes as a function of time, hydraulic diffusivity D can be estimated by finding a parabola from Eq. (4) that represents the upper envelope of all points in the time–depth plot (Shapiro *et al.* 1997).

Fig. 8 plots focal depth over time for the earthquake series in Muotathal and Riemenstalden. We do not separate between the two regions because the number of events is relatively low, and because the regions are not far apart. Furthermore, they show a similar geology (Karst areas), which suggests that hydraulic diffusivity may not be very different. We chose two different starting times for the plots: (1) 08/19/2005 at 16:00 and (2) 08/21/2005 at 10:00. Rainfall started on 08/19/2005 at 16:00 with a small maximum and a break until 08/21/2005 at 10:00 when the actual rainfall event started (Fig. 3). We find hydraulic diffusivities of $D = 0.10$ and 0.20 m s^{-2} for the earlier start time and the later start time, respectively (Fig. 8). Most of the earthquakes occurred at shallow depths (<5 km) and were of small magnitudes. Consequently, estimated errors in focal depth were large as shown by large error bars in Fig. 8. Taking these error bounds into account hydraulic diffusivities can range over one order of magnitude from $D = 0.01$ to 0.15 m s^{-2} and from $D = 0.05$ to 0.50 m s^{-2} for the earlier start time and the later start time, respectively (Fig. 8).

Estimated hydraulic diffusivities are known to vary over several orders of magnitudes. Based on the evolution of reservoir induced seismicity, Talwani & Acree (1984) estimated hydraulic diffusivities in the range from 0.5 to 50.0 m^2 s^{-1}. Hydraulic diffusivities in crystalline rocks estimated from fluid-injection experiments at depths between 2.0 and 9.0 km depth range from 0.05 to 1.0 m^2 s^{-1} (Zoback & Harjes 1997; Shapiro *et al.* 2002). Finally, hydraulic diffusivities inferred from seismicity induced by seasonal groundwater recharge or by rainfall range from 0.1 to 1 m^2 s^{-1} (Roth *et al.* 1992; Saar & Manga 2003; Kraft *et al.* 2006). Our values fit well in this range, strongly supporting the idea that observed seismicity was triggered by the large amount of rainfall.

DISCUSSION AND CONCLUSIONS

We found good evidence that a series of earthquakes in central Switzerland was triggered by heavy rainfall. Seismicity and rainfall show a clear correlation in time and space. Earthquakes occurred at the end of a 3-d period of exceptional heavy rainfall on 2005 August 23, and they clustered in regions that received some of the highest rainfall (Fig. 1). In our preferred model, an increase in fluid pressure at the surface due to a large amount of rain leads to a local increase in pore fluid pressure at depth. An increase in pore fluid pressure will reduce the shear strength of a porous medium by counteracting normal stress and, at the end, provoke failure. A viable mechanism that explains the migration of a pressure pulse to greater depth is diffusion, which is governed by the hydraulic diffusivity of the medium. We estimated hydraulic diffusivity D based on the temporal evolution of focal depths for the region, that experienced the highest triggered seismicity in central Switzerland (Muothatal and Riemenstalden). Our best-fitting value of $D = 0.10$–0.20 m^2 s^{-1} fits well in the range of hydraulic diffusivities found for similar studies (Roth *et al.* 1992; Saar & Manga 2003; Kraft *et al.* 2006). This further supports our model of pore-pressure diffusion and the associated increase in local pore pressure being the main triggering mechanism.

Our estimate of D is based on a simplified hydrological model and can only represent a first order approximation. Hence, the obtained value of D can only be understood as an average over the studied volume. D might not be constant in time because dynamic
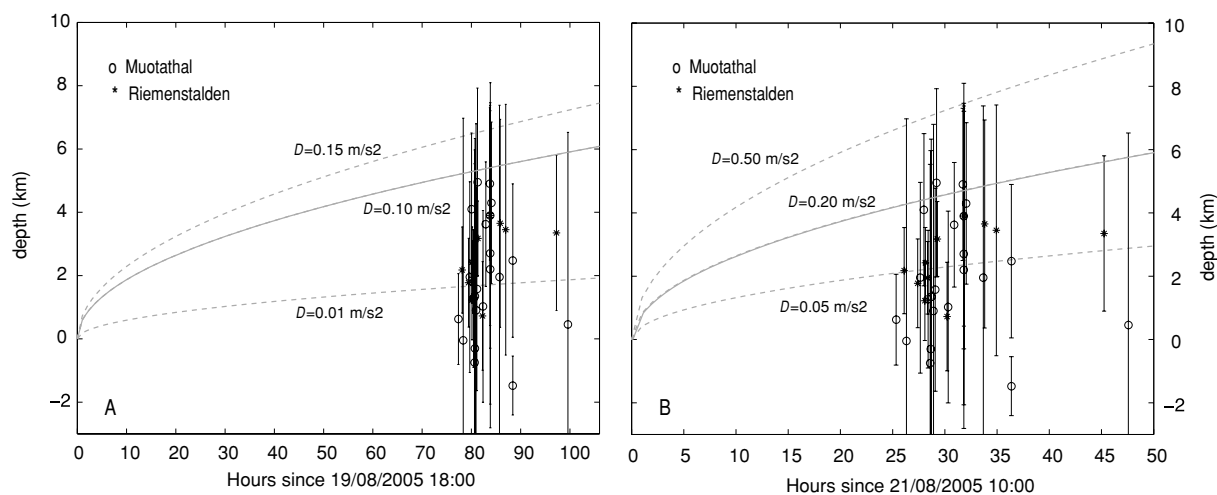
Figure 8. Focal depth versus time plot for earthquakes triggered in the Muotathal (circles) and Riemenstalden (stars) region. Time is in hours since (a) 08/19/2005 12:00 and since (b) 08/21/2005 10:00. Error in focal depth is shown by error bars as estimated from the 68 per cent confidence ellipsoid. Best fitting parabolas are shown for located focal depth plus error (dashed), located focal depth (solid), and located focal depth minus error (dashed). Hydraulic diffusivities D are labelled for each parabola. Depth of 0 km corresponds to 2 km above sea level (average elevation of Earth surface in the region). See text for more information on how to estimate D from focal depth versus time plots.

rupture can change porosity and permeability (Miller *et al.* 2004). In a real geological setting, D has to be calculated in the form of an anisotropic tensor (Rothert & Shapiro 2003) which is likely highly heterogeneous. Furthermore, the Muothatal and Riemenstalden regions are dominated by Karst geology with large open fractures. These fractures may act as pathways, allowing fluids to migrate to greater depth much faster and much more efficiently than modelled by simple pore-pressure diffusion. On the other hand, it should be noted that our estimated hydraulic diffusivities vary over one order of magnitude if the appropriate error in focal depth is taken in consideration (Fig. 8). Most of the earthquakes were of small magnitudes ($M < 2$) and, consequently, only observed at a low number of stations (<6). This in conjunction with very shallow focal depths (<5 km) yield large uncertainties in focal depths (Fig. 6). Therefore, a more detailed or more realistic hydrological interpretation is beyond the limits of our data set. Studies of induced seismicity by fluid injection in boreholes are much more suitable for these kind of studies since monitoring networks are of much higher quality for these experiments, as compared to nation-wide networks for routine seismicity monitoring.

In our interpretation we assumed that induced pore-pressure variations can cause stress changes large enough to trigger earthquakes. Our simplistic approach does not allow to model stress changes caused by pore-pressure variations. For a very similar tectonic setting at Mt Hochstaufen, SE Germany, Hainzl *et al.* (2006) combined the solution of the diffusion equation describing the evolution of fluid mass alteration per unit volume with the framework of rate-state friction (Dieterich 1994) to quantify the effects of pore pressure changes on seismicity. Using high-quality seismic and meteorological data from dense networks they concluded that stress changes in the order of 100 Pa are sufficient to trigger earthquakes. These stress changes are several orders of magnitude smaller than observed for the bulk of induced seismicity in fluid injection experiments, which are in the order of 1 MPa (Zoback & Harjes 1997). At the same time, it is generally accepted that many faults are near critically stressed and that small stress changes may be sufficient to provoke failure on pre-existing faults (Townend & Zoback 2000). The regions of Riemenstalden and Muotathal are located within the Helvetic nappes, which have been extensively folded and fractured during crustal shortening (Fig. 5). Moreover, earthquakes triggered by the rainfall occurred close to hypocentre locations of past earthquakes, with similar magnitudes and focal depths (Fig. 6). This supports the idea that these earthquakes occurred on existing faults that were critically stressed. In other words, the earthquakes were 'clock-advanced' they would have happened sooner or later. The fact that only a few regions in central Switzerland showed an increase in seismicity following the unusual rainfall event, although the amount of rainfall was equally high (Fig. 1), also strengthens this idea. Some of the regions that did not experience earthquake triggering, such as the Molasse basin of the Alpine foreland, are known to be seismically relatively quiet indicating that existing faults may not be critically stressed (Baer *et al.* 2003).

Examples of earthquake triggering by intense rainfall or seasonal groundwater recharge are still rare. For Switzerland, a weak correlation was previously found between long periods of intense precipitation and an increase in seismicity (Roth *et al.* 1992). However, these observations are not comparable in magnitude to ours. Clearly, the amount of rainfall in the time period of August 19–22, 2005, was exceptionally. The statistical recurrence rate for such an event is more than 300 yr (Meteoswiss 2005, personal communication). Whether previous rainfall events were not strong enough to trigger earthquakes is an important question. It is likely that a certain

threshold may exist above which earthquakes can be triggered by rainfall. This threshold will depend not only on the amount of rainfall but also on crustal stress conditions. Hence, a systematic study of rainfall related earthquake triggering would provide important insights into the state of stress of the upper crust. We are not aware of a similar increase in seismicity following other periods of intense rainfall. However, smaller increases in seismicity could have occurred undetected because magnitudes of triggered earthquakes are small and at the lower end of the detection threshold of the Swiss Digital Seismic Network. A systematic study of rainfall related earthquake triggering would need a denser array of seismic stations and more sophisticated statistical analysis, which is beyond the scope of this study.

REFERENCES

Aki, K. *et al.*, 1982. Interpretation of seismic data from hydraulic fracturing experiments at the Fenton-Hill, New-Mexico, Hot Dry Rock Geothermal Site, *J. geophys. Res.,* **87**(NB2), 936–944.

Baer, M. *et al.*, 2003. Earthquakes in Switzerland and surrounding regions during 2002, *Eclogae Geologicae Helvetiae,* **96**(2), 313–324.

Boegli, A., 1970. Das Hoelloch und sein Karst, *Stalactite: Suppl.* **4a**.

Dieterich, J., 1994. A constitutive law for rate of earthquake production and its application to earthquake clustering, *J. Geophys. Res.-Solid Earth,* **99**(B2), 2601–2618.

Gupta, H.K., 2002. A review of recent studies of triggered earthquakes by artificial water reservoirs with special emphasis on earthquakes in Koyna, India, *Earth-Sci. Rev.,* **58**(3–4), 279–310.

Hainzl, S., Kraft, T., Wassermann, J., Igel, H. & Schmedes, E., 2006. Evidence for rainfall-triggered earthquake activity, *Geophys. Res. Lett.,* **33**(19), doi: 10.1029/2006GL027642.

Husen, S., Kissling, E., Deichmann, N., Wiemer, S., Giardini, D. & Baer, M., 2003. Probabilistic earthquake location in complex three-dimensional velocity models: application to Switzerland, *J. Geophys. Res.-Solid Earth,* **108**(B2), 2077, doi: 10.1029/2002JB001778.

Husen, S., Wiemer, S. & Smith, R.B., 2004. Remotely triggered seismicity in the Yellowstone National Park region by the 2002 M-W 7.9 Denali fault earthquake, Alaska, *Bull. Seismol. Soc. Am.,* **94**(6), S317–S331.

Jimenez, M.J. & Garcia-Fernandez, M., 2000. Occurrence of shallow earthquakes following periods of intense rainfall in Tenerife, Canary Islands, *J. Volcanol. Geother. Res.,* **103**(1–4), 463–468.

Kraft, T., Wassermann, J., Schmedes, E. & Igel, H., 2006. Meteorological triggering of earthquake swarms at Mt. Hochstaufen, SE-Germany, *Tectonophysics,* **424**(3–4), 245–258.

Lomax, A., Virieux, J., Volant, P. & Berge-Thierry, C., 2000. Probabilistic earthquake location in 3D and layered models, in *Advances in Seismic Event Location,* pp. 101–134, eds Thurber, C.H. & Rabinowitz, N., Kluwer Academic Publishers, Dordrecht/Boston/London.

Miller, S.A., Collettini, C., Chiaraluce, L., Cocco, M., Barchi, M. & Kaus, B.J.P. , 2004. Aftershocks driven by a high-pressure CO_2 source at depth, *Nature,* **427**(6976), 724–727.

Nur, A. & Booker, J.R., 1972. Aftershocks caused by pore fluid-flow, *Science,* **175**(4024), 885–887.

Parotidis, M., Shapiro, S.A. & Rothert, E., 2005. Evidence for triggering of the Vogtland swarms 2000 by pore pressure diffusion, *J. Geophys. Res.-Solid Earth,* **110**(B5), doi: 10.1029/2004JB003267.

Phillips, W.S., 2000. Precise microearthquake locations and fluid flow in the geothermal reservoir at Soultz-sous-Forets, France, *Bull. Seismol. Soc. Am.,* **90**(1), 212–228.

Prejean, S.G. *et al.*, 2004. Remotely triggered seismicity on the United States west coast following the M-W 7.9 Denali fault earthquake, *Bull. Seismol. Soc. Am.,* **94**(6), S348–S359.

Roth, P., Pavoni, N. & Deichmann, N., 1992. Seismotectonics of the Eastern Swiss Alps and evidence for precipitation-induced variations of seismic activity, *Tectonophysics,* **207**(1–2), 183–197.

Rothert, E. & Shapiro, S.A., 2003. Microseismic monitoring of borehole fluid injections: data modeling and inversion for hydraulic properties of rocks, *Geophysics,* **68**(2), 685–689.

Rowe, C.A., Aster, R.C., Borchers, B. & Young, C.J., 2002. An automatic, adaptive algorithm for refining phase picks in large seismic data sets, *Bull. Seismol. Soc. Am.,* **92**(5), 1660–1674.

Saar, M.O. & Manga, M., 2003. Seismicity induced by seasonal groundwater recharge at Mt. Hood, Oregon, *Earth Planet. Sci. Lett.,* **214**(3–4), 605–618.

Schmid, S.M. & Kissling, E., 2000. The arc of the western Alps in the light of geophysical data on deep crustal structure, *Tectonics,* **19**(1), 62–85.

Schmid, S.M., Fugenschuh, B., Kissling, E. & Schuster, R., 2004. Tectonic map and overall architecture of the Alpine orogen, *Eclogae Geol. Helv.,* **97**(1), 93–117.

Shapiro, S.A., Huenges, E. & Borm, G., 1997. Estimating the crust permeability from fluid-injection-induced seismic emission at the KTB site, *Geophys. J. Int.,* **131**(2), F15–F18.

Shapiro, S.A., Rothert, E., Rath, V. & Rindschwentner, J., 2002. Characterization of fluid transport properties of reservoirs using induced microseismicity, *Geophysics,* **67**(1), 212–220.

Shapiro, S.A., Rentsch, S. & Rothert, E., 2005. Fluid-induced seismicity: theory, modeling, and applications, *J. Eng. Mech.-Asce,* **131**(9), 947–952.

Swiss Hydrological Survey, 2007. Hydrologisches Jahrbuch 2005, *Federal Office for the Enviroment*.

Talwani, P., 1997. On the nature of reservoir-induced seismicity, *Pure Appl. Geophys.,* **150**(3–4), 473–492.

Talwani, P. & Acree, S., 1984. Pore pressure diffusion and the mechanism of reservoir-induced seismicity, *Pure Appl. Geophys.,* **122**(6), 947–965.

Townend, J. & Zoback, M.D., 2000. How faulting keeps the crust strong, *Geology,* **28**(5), 399–402.

Wang, H.F., 2000. *Theory of Linear Poroelasticity with Applications to Geomechanics and Hydrogeology,* Princeton University Press, Princeton, NJ, 287 pp.

Wildberger, A. & Baettig, G., in press. Ein Vergleich des Hölloch-Hochwassers vom August 2005mit seinen Vorgängern, *Stalactite,* **57**(2), in press.

Zoback, M.D. & Harjes, H.P., 1997. Injection-induced earthquakes and crustal stress at 9 km depth at the KTB deep drilling site, Germany, *J. Geophys. Res.-Solid Earth,* **102**(B8), 18 477–18 491.